

Fabrication of Wear and Corrosion Resisting G3 Alloy-like Coating on P110 Steel by Double Glow Plasma Alloying

Wei Tian^{1,2}, Wenhai Yu², Naiming Lin^{1,*}, Jiaojuan Zou¹, Junwen Guo¹, Hongyan Zhang¹, Peng Zhou¹, Ruizhen Xie¹, Yong Ma¹, Zhenxia Wang¹, Xiaofei Yao³, Pengju Han⁴, Xiaoping Liu¹, Bin Tang¹

¹ Research Institute of Surface Engineering, Taiyuan University of Technology, Taiyuan, 030024, P. R. China

² China United Northwest Institute for Engineering & Research, Xi'an, 710082, P. R. China

³ School of Materials and Chemical Engineering, Xi'an Technological University, Xi'an, 710032, P. R. China

⁴ Department of Civil Engineering, Taiyuan University of Technology, Taiyuan, 030024, P. R. China

*E-mail: lnmlz33@126.com

Received: 10 April 2015 / Accepted: 15 May 2015 / Published: 24 June 2015

There is a need for oil casing tubes to resist both wear and corrosion attacks during operation. In the present work, a G3 alloy-like coating has been formed on P110 oil casing tube steel via double glow plasma surface alloying using a G3 alloy source electrode to improve its surface performance and prolong its service life-time. X-ray diffraction (XRD), scanning electron microscope (SEM), optical microscope (OM), glow discharge optical emission spectroscopy (GDOES) and micro hardness tester were employed to analysis the phase constitution, surface morphology/composition, cross-sectional microstructure, element distribution and surface hardness value of the G3 alloy-like coating. The wear resistance of the G3 alloy-like coating was measured by reciprocating type tribometer under dry sliding against GCr15 steel and Si₃N₄ counterparts. Electrochemical measurements, open circuit potential and potentiodynamic polarization were conducted in some CO₂-saturated simulated oilfield brine to evaluate the anti-corrosion property of the G3 alloy-like coating. The results revealed that the received G3 alloy-like coating was uniform and compact. The G3 alloy-like coating with higher surface hardness had significantly improved the anti-wear property of P110 steel. The G3 alloy-like coating had better corrosion resistance revealing by higher open circuit potential and lower corrosion current density as compared with P110 steel. The formation of G3 alloy-like coating has made it possible to enhance the anti-wear property and corrosion resistance of P110 steel.

Keywords: wear; corrosion; G3 alloy; coating; oil casing tube; P110 steel; double glow plasma surface alloying

1. INTRODUCTION

Human culture has recognized the importance of materials degradation and protection ever since the very beginning of civilization [1]. In nowadays, material engineers are constantly confronted with the challenge to design and produce new materials that are both wear and corrosion resistant over wide range of modern industrial environments and applications [2]. One way of achieving this is via surface modification technique involving coating formulations through compositional modifications as well as improved surface processing techniques [2]. It is well accepted that surface modification takes the advantage of offering a compromise between the performance against degradations and the cost with promising properties to prevent or minimize the wastage of materials [3].

The rapid economic growth and industrial development around the world have contributed to huge consumption of oil/gas over the past decades, and much more oil/gas wells are required to exploit [4]. Petroleum tube is a key structural unit of an oil well. It takes about 1/3 of the whole cost of developing an oil well, and the oil casing tube holds almost 3/4 of the entire petroleum tube consumes [4, 5]. The oil casing tubes are prone to degradation and failure that caused by wear and corrosion when they are operated in oil/gas wells [4]. It was reported that oil casing tube directly influence the life-time of an oil well, the oil well might determine the oil field service time [4]. According to the investigations and understandings about corrosion of oil casing tubes, corrosion protection methods, such as application of anticorrosion alloy, injection of inhibitor, cathode protection and surface treatment have been used [6]. Actually using anticorrosion alloy tubes is the most effective way to guarantee high efficient and safe production, e.g. Ni-base alloys: Inconel 625, Inconel 718, G3 and Incoloy 825 [7]. However, the mentioned above anticorrosion alloy contains large amounts of noble metals (*e g*, Ni, Cr, Mo), and this would bring out the increasing in petroleum production cost [5]. In many engineering applications, surface performance has significant impacts on the life of metallic work pieces [8]. Most types of material degradation, such as wear, corrosion/oxidation and fatigue/fracture are often generated on the surfaces of engineering components. However surface modification techniques can overcome the aforementioned problems [9].

In the present work, attempts were therefore conducted to simultaneously impart P110 steel high wear and corrosion resistance by fabricating a G3 alloy-like coating via double glow plasma surface alloying (DGPSA) [10]. The microstructural characterizations and surface hardness of the obtained G3 alloy-like coating were systemically investigated. The anti-wear property and corrosion resistance of the G3 alloy-like coating and P110 steel were comparatively estimated.

2. EXPERIMENTAL PROCEDURE

2.1 Processing

P110 steel substrate materials were prepared from a P110 steel tube in the size of $25 \times 12 \times 5$ mm³. G3 alloy source electrode was prepared from a G3 alloy tube. Chemical compositions of P110 steel and G3 alloy are suggested in Table 1 [11, 12]. Before plasma surface alloying treatment, all the P110 steel specimens were mechanically ground using emery papers and degreased in acetone. The

DGPSA treatment was conducted on independent equipment. Figure 1 suggests the schematic diagram of DGPSA apparatus. The technological principle of DGPSA had been described in other published papers [10, 13–18]. In the present work, argon (Ar) gas was chosen as the carrier gas. Firstly, the P110 steel specimens were subjected to ion bombardment in an Ar glow discharge for 30 min. The DGPSA process was performed at target (source electrode) voltages ranging in $-750\sim-650$ V under a temperature range of $950\sim1000$ °C, P110 steel substrate (work piece) was conducted at voltages between $-700\sim-500$ V to heat the P110 steel substrate up to a temperature of 900 °C, the distance between the source electrode and the work piece was 15 mm. The gas pressure in the chamber was kept about $35\sim40$ Pa through the DGPSA process. The whole DGPSA duration was of 4 h. Then the DGPSA treated P110 steel sample was cooled under the argon flow in the vacuum chamber [13].

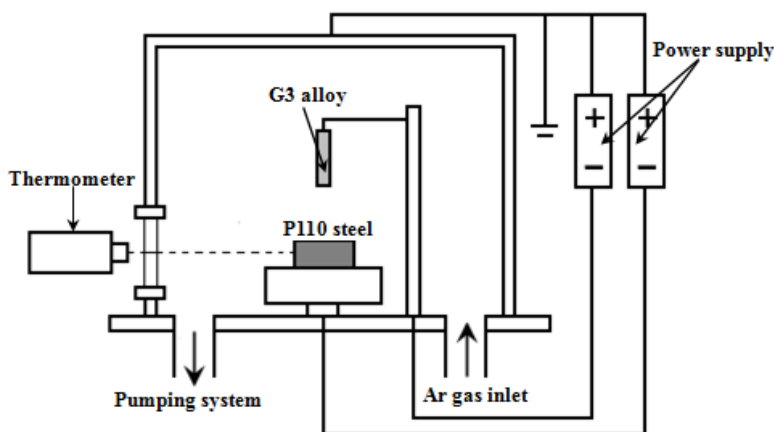


Figure 1. Schematic diagram of DGPSA apparatus

Table 1. Chemical compositions of P110 steel and G3 alloy (Wt. %)

| Element | C | Si | Mn | P | S | Cr | Ni | Mo | Cu | Nb | V | Ti | Fe |
|------------|-------|------|------|-------|-------|-------|---------|-------|-------|------|-------|-------|---------|
| P110 steel | 0.26 | 0.19 | 1.37 | 0.009 | 0.004 | 0.148 | 0.028 | 0.013 | 0.019 | 0.06 | 0.006 | 0.011 | balance |
| G3 alloy | 0.009 | 0.12 | 0.51 | 0.007 | 0.001 | 22.05 | balance | 6.79 | 1.76 | 0.10 | / | / | 20.02 |

2.2 Characterizations and testing

Microstructural analyses and thickness measurements of a G3 alloy-like coating were carried out under the OM. Nital-etched micro-section perpendicular to the surface of the sample was examined. The elemental composition profile along the thickness to the G3 alloy-like coating was examined using GDOES. The surface morphology of the obtained coating was investigated by employ of SEM. The phase constitution of the G3 coating was evaluated using XRD. A micro-hardness tester was used to measure the surface hardness of G3 alloy-like coating and P110 steel via a Vickers indenter.

MFT-R4000 reciprocatory type friction-wear testing machine was used to estimate the wear resistance of P110 steel and G3 alloy-like coating. The atmospheric condition in the laboratory has

involved a temperature of 298 K and a relative humidity of 40~45 %. GCr15 steel and Si₃N₄ balls with the size of Φ 5 mm were selected as the counterparts. All the tests were performed under the following conditions: by wearing against counter balls with a reciprocatory displacement of 5 mm, a load of 10 N, a sliding velocity of 2 Hz for 30 min. An analytical balance with an accuracy of 0.01 mg was used to get the mass losses of the tested samples. The worn surfaces of the tested samples were also observed using SEM [19].

The corrosion resistance of the G3 alloy-like coating was examined by electrochemical measurements, open circuit potential (OCP) and potentiodynamic polarization [11, 20, 21]. The corrosion medium, CO₂-saturated simulated oilfield brine was prepared from reagent grade chemical and distilled water [22, 23]. The corrosion solution was bubbled using nitrogen gas (N₂) for 4 h to deaerate and kept CO₂ passing through for 4 h. The electrochemical experiments were performed with the CS350 electrochemical measurement system, and a traditional three-electrode cell has been applied to perform the mentioned electrochemical tests with a temperature of 303 K throughout the experiment. The reference electrode was a saturated calomel electrode (SCE) and the counter electrode (CE) was a platinum plate. The specimens of bare P110 steel and G3 alloy-like coating were used as the working electrode (WE) [22, 23]. The OCP measurements were started after the each sample was put into the corrosion medium, and the total time was 3600 s. The potentiodynamic polarization of the sample was swept at a rate of 1 mV/s.

3. RESULTS AND DISCUSSION

3.1 Microstructural characterizations

XRD diffract gram of the obtained coating is suggested in Figure 2, which can help to elucidate the material transformations that had taken place in the P110 steel surface. Seen from Figure 2, the diffraction peaks of the coating rather close to the G3 alloy source electrode, it has indicated the formation of G3 alloy-like coating on P110 steel by DGPSA.

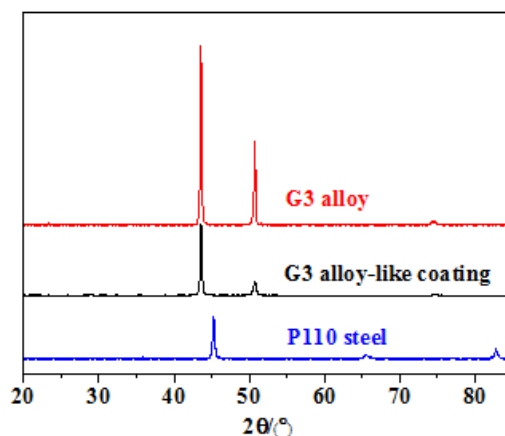


Figure 2. XRD pattern of the G3 alloy, G3 alloy-like coating and P110 steel

Figure 3 presents the surface morphology (a) and composition (b) of the G3 alloy-like coating. As exhibited in Figure 3, the G3 alloy-like coating is uniform and continuous. Some protuberances distribute on the G3 alloy-like coating surface. The protuberances might be resulted from the local fusion of G3 alloy target which was induced by point discharge [10]. The surface compositions of the G3 alloy-like coating and G3 alloy source electrode have further confirmed the formation of G3 alloy-like coating by surface EDS scan, as shown in Figure 3(b) and Figure 3(c). As the G3 alloy source electrode was suspended by thin Mo bar in DGPSA, Mo atoms were bombarded out from the G3 alloy source electrode and Mo bar which has resulted higher in Mo on the surface G3 alloy-like coating than that of G3 alloy source electrode.

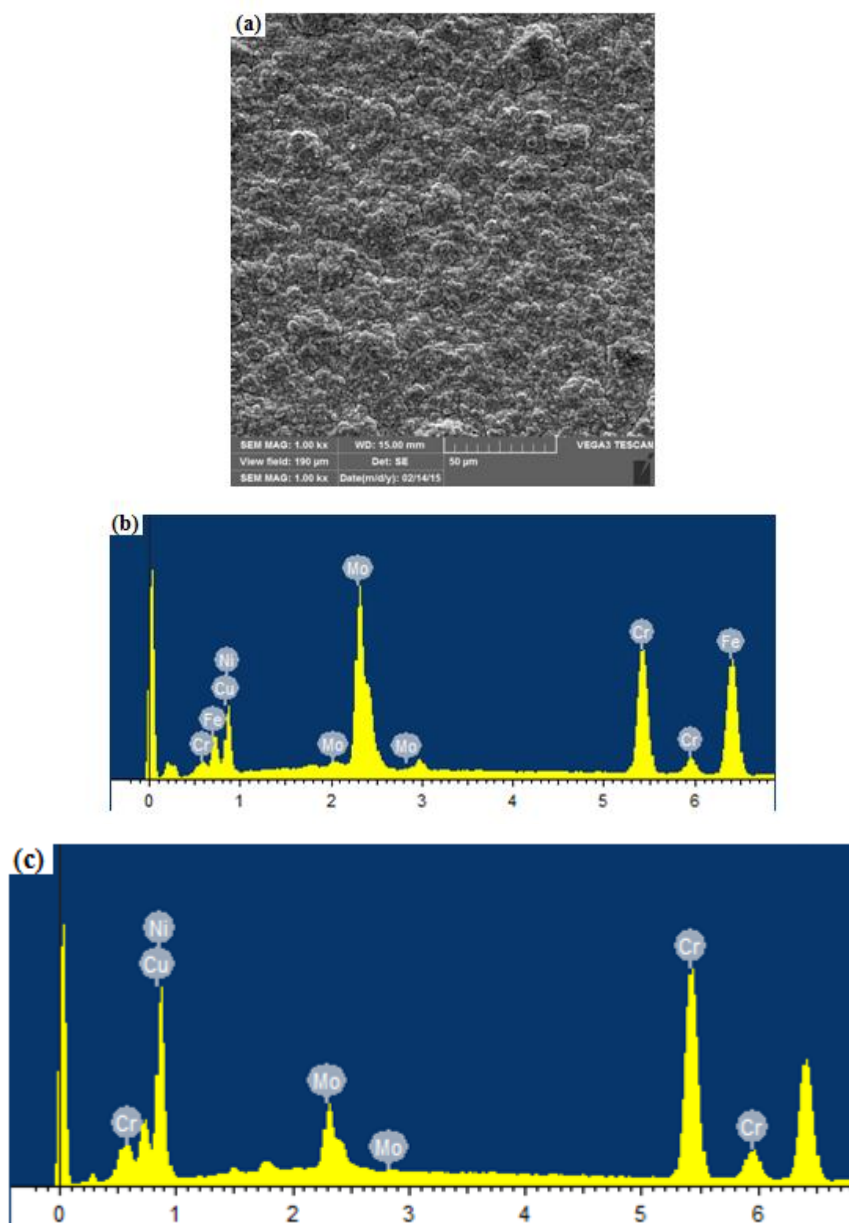


Figure 3. Surface morphology (a) and composition (b) of G3 alloy-like coating, composition of G3 alloy (c)

The microstructure of the G3 alloy-like coating on P110 steel was analyzed under an OM on transverse nital-etched micro-section. A bright, non-etched layer with an estimated thickness of 35 μm was observed according to the measuring scale, and it was clearly separated from the P110 steel substrate (Figure 4(a)). GDOES analysis results is shown in Figure 4(b), it is found that the concentration of Ni and Cr decreased gradually, the composition of Fe increased from the surface to inside [13]. This gradient distributing character of Ni, Cr and Fe elements in the coating has been found to be helpful to enhance the bonding strength at the interface of the coating and the substrate [17]. It can be seen in Figure 4(b) that the G3 alloy-like coating reached a thickness of about 35 μm .

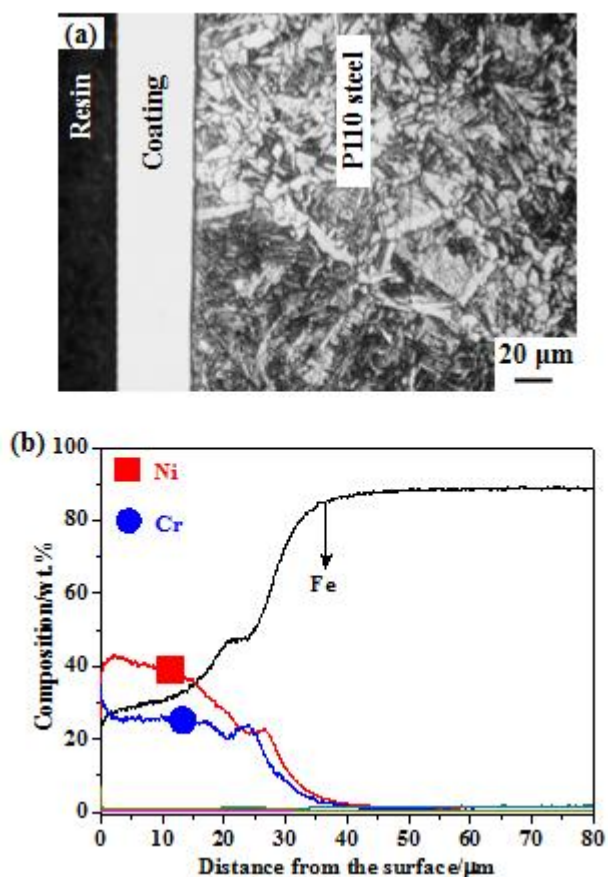


Figure 4. Cross-sectional microstructure (a) and composition profile (b) of G3 alloy-like coating

3.2 Wear resistance

According to the measuring points on the surfaces of bare P110 steel and G3 alloy-like coating, surface hardness column charts were created as shown in Figure 5. The G3 alloy-like coating has higher hardness value than P110 steel. The higher hardness on the G3 alloy-like coating surface can also enhance the anti-wear property of P110 steel [24]. Figure 6 illuminates the friction coefficients of the G3 alloy-like coatings and the P110 steel substrates and against GCr15 and Si_3N_4 . Seen from Figure 6, it is found that the friction coefficients of the P110 steel substrate are lower than those of the G3 alloy-like coating. The distinctions can be explained from the following aspects: firstly, the

ground P110 steel is smooth, and the P110 steel is not as hard as the GCr15 and Si₃N₄ balls, the friction force between the P110 steel and the counterparts is low; secondly, the protuberances on the coated surface which have an effect on the surface roughness, increased the friction coefficients; thirdly, adhesion is prone to occur between a metal-metal friction interface as compared with a ceramic-metal friction interface, hence the friction coefficients against GCr15 are more fluctuated than those of against Si₃N₄ [25, 26].

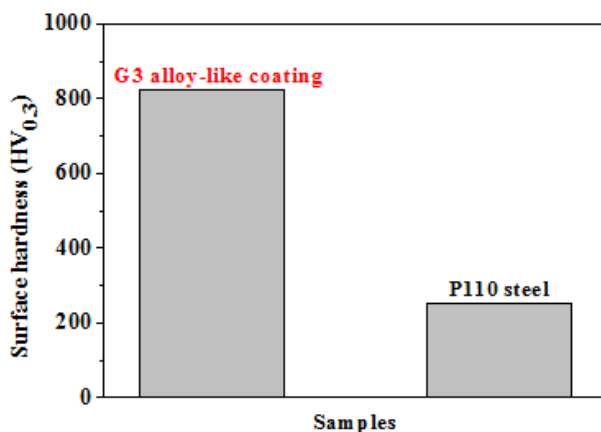


Figure 5. Surface micro hardness values of tested samples

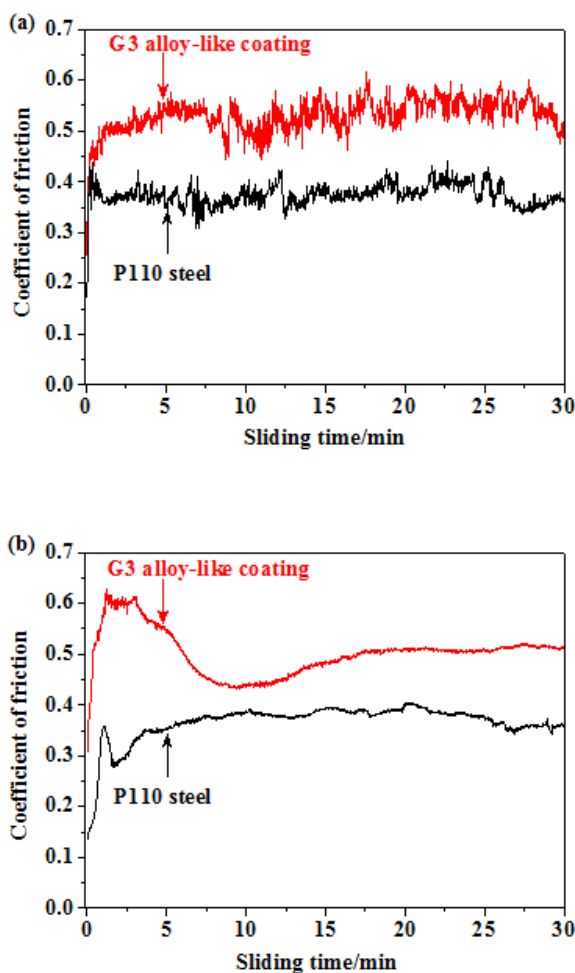


Figure 6. Coefficients of friction of tested samples sliding against GCr15 (a) and Si₃N₄ (b)

Figure 7 compares the differences in mass loss between P110 steel substrates and G3 alloy-like coatings after dry sliding. It is obviously that the mass losses of the G3 alloy-like coatings (0.02667 mg and 0.01667 mg) were lower than P110 steel substrates (0.09667 mg and 0.04333 mg). The lower mass losses of G3 alloy-like coating compared with P110 steel was mainly due to the improvement in surface hardness degree of the G3 alloy-like coating and the high metallurgical bonding strength [25, 26]. Therefore the P110 steel showed higher mass losses than those of the G3 alloy-like coating. It is allowed to draw a conclusion that the G3 alloy-like coating had significantly improve the wear resistance of P110 steel.

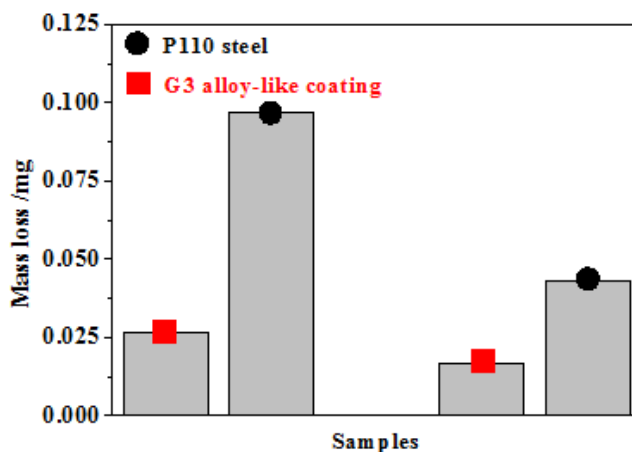


Figure 7. Mass losses of tested samples sliding against GCr15 and Si₃N₄

Figure 8 displays the whole and enlarged SEM images of wear traces for G3 alloy-like coating and P110 steel after dry sliding against GCr15. EDS analyses for zone 1 and zone 2 in Figure 8(b) are suggested in Table 2. Zone 1 in grey color reveals high Cr, Ni and Mo content, which means the G3 alloy-like coating was not worn through. Zone 2 in dark color with higher O and Fe contents than zone 1 might have formed in the transfers from GCr15 counterpart. The concentrations of O in zones 1 and 2 as revealed in Table 2 had proved oxidation reactions took place, it was owing to the chemical reaction of the metal to oxidize. Combining with the mass loss results, the wear mode of G3 alloy-like coating mainly was the transfer of counterpart to the G3 alloy-like coating associated with oxidation wear.

Table 2. EDS results of worn G3 alloy-like coating sliding against GCr15

| Element (Wt. %) | O | Cr | Fe | Ni | Cu | Mo |
|-----------------|-------|-------|-------|-------|------|-------|
| Zone-1 | 14.77 | 13.65 | 40.46 | 18.22 | 0.06 | 12.85 |
| Zone -2 | 37.54 | 3.45 | 53.43 | 3.14 | 0.01 | 2.42 |

As shown in Figure 8(d), the worn P110 steel showed very rough surface, adhesive and abrasive marks were noticeable. There was high chemical affinity between P110 steel and GCr15 steel, thus cold welding or adhesion was prone to happen between the friction interface. However, this link could be broken by relative sliding of the friction couples [25, 26]. Adhesive wear occurred, which was

demonstrated by adhesive built-up (zone 2) and detected by EDS in Table 3. The presence of O in zone 1 and zone 2 has revealed the oxidation occurred during dry sliding [25, 26]. The main wear mode of P110 steel was adhesive wear combined with oxidation wear and abrasive wear.

Table 3. EDS results of worn P110 steel sliding against GCr15

| Element (Wt. %) | C | O | Mn | Fe |
|-----------------|------|-------|------|-------|
| Zone-1 | 3.37 | 7.08 | 1.23 | 88.32 |
| Zone -2 | 2.91 | 37.92 | / | 59.17 |

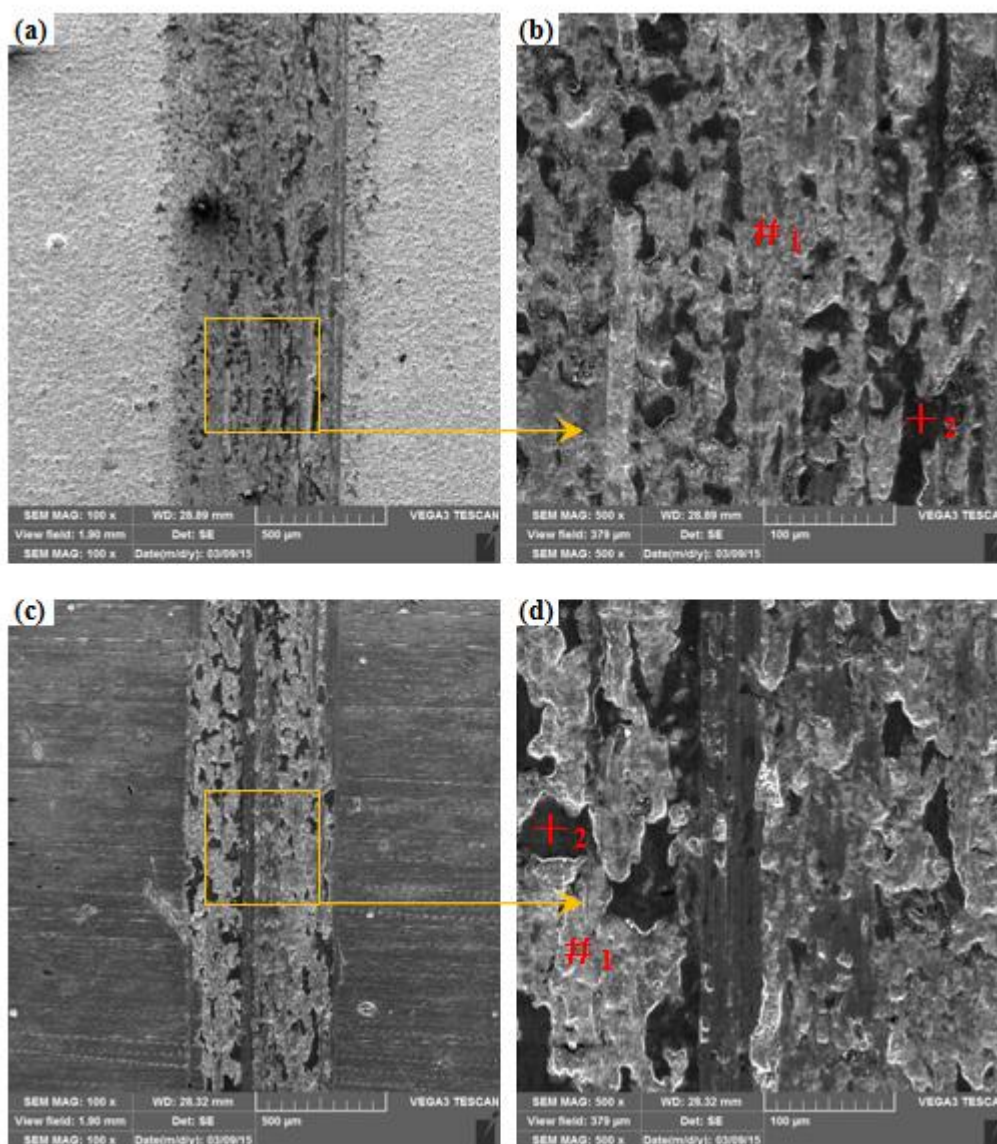


Figure 8. Wear traces of G3 alloy-like coating (a) , (b) and P110 steel (c), (d) sliding against GCr15

Table 4. EDS results of worn G3 alloy-like coating sliding against Si₃N₄

| Element (Wt. %) | N | O | Si | Cr | Fe | Ni | Cu | Mo |
|-----------------|------|-------|------|-------|-------|-------|------|-------|
| Zone-1 | 0.21 | 7.18 | 0.22 | 20.85 | 27.85 | 19.12 | 0.06 | 24.51 |
| Zone -2 | 1.68 | 40.42 | 1.08 | 13.33 | 16.51 | 12.96 | 0.02 | 13.98 |

Table 5. EDS results of worn P110 steel sliding against Si₃N₄

| Element (Wt. %) | C | N | O | Si | Mn | Fe |
|-----------------|------|------|-------|------|------|-------|
| Zone-1 | 2.35 | 0.78 | 12.62 | 0.9 | 1.24 | 82.12 |
| Zone -2 | 1.94 | 1.33 | 30.77 | 1.98 | / | 63.99 |

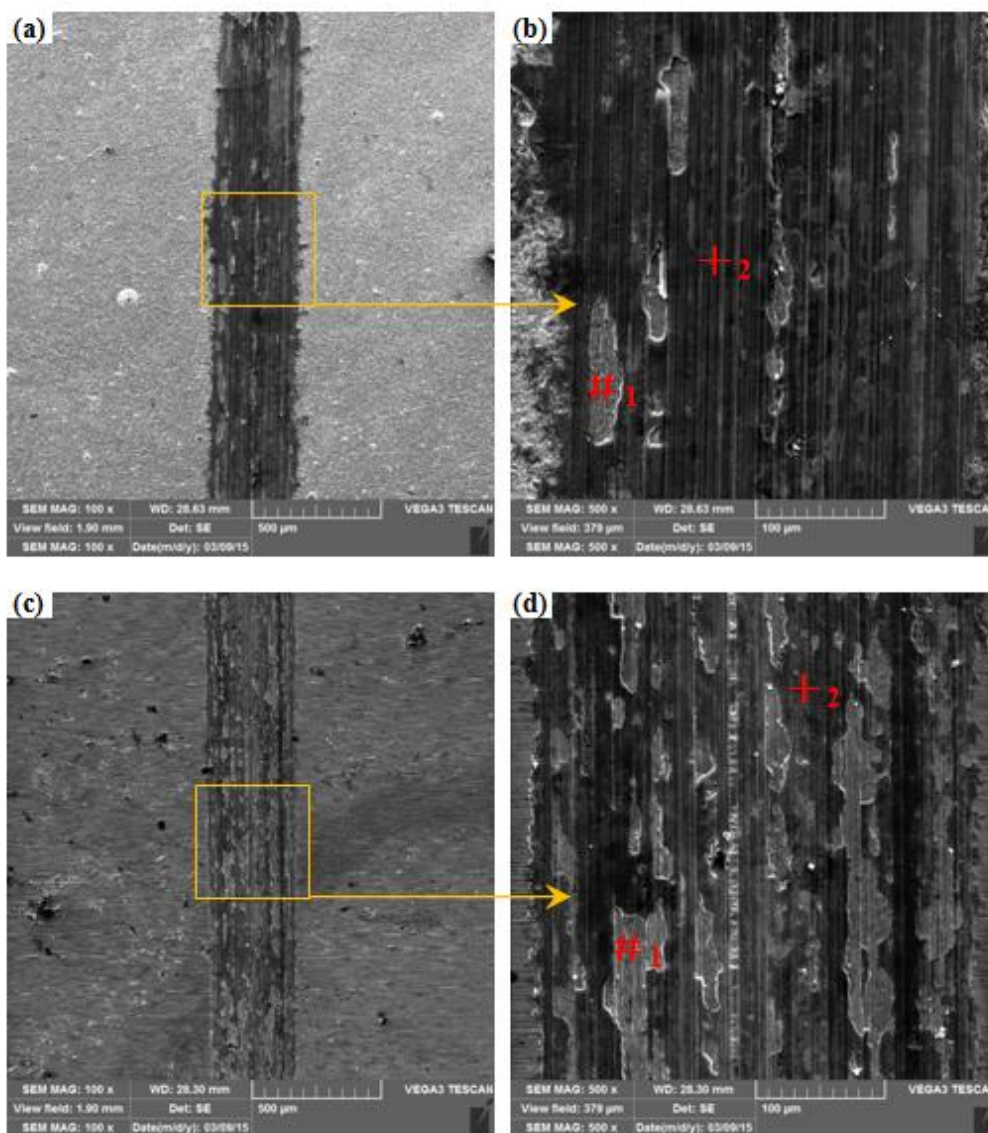


Figure 9. Wear traces of G3 alloy-like coating (a), (b) and P110 steel (c), (d) sliding against Si₃N₄

When sliding against Si_3N_4 , G3 alloy-like coating also exhibited promising wear resistance. Figure 9 reveals the wear characteristics of G3 alloy-like coating and P110 steel. EDS analysis of the worn surfaces was also conducted to distinguish the wear mechanisms of the tested samples. Table 4 and Table 5 show the EDS analysis results. Seen from Figure 9(b), two kinds of distinct zones with different color on worn G3 alloy-like coating surface can be found; meanwhile slim grooves are obvious in the wear trace [25, 26]. Although Si_3N_4 is harder than the obtained coating, the elemental compositions of point 1 in Table 4 reveals the G3 alloy-like coating was not worn through. In addition, EDS analysis of point 2 in Table 4 indicates the phenomena of oxidation [25, 26]. The main wear mechanism of the G3 alloy-like coating was micro-scratching associated with oxidation wear.

As shown in Figure 9(b) and Figure 9(d), the Si_3N_4 ball had produced much heavier wearing on P110 steel than that on the G3 alloy-like coating in sliding. EDS has provided promising explanation of the worn trace in Figure 9(d) as tabulated in Table 5, point 2 with plentiful O clearly confirms the friction-induced oxidation had generated on P110 steel surface during sliding. The formed oxide layer could protect P110 steel from further serious surface destroy. The oxide layer could not resist the ground of Si_3N_4 ball and had been smashed into tiny wear debris, which led to the exposure of fresh P110 steel substrate as detected by EDS [25, 26]. The oxide layer was involved in the friction and was dispersed into small abrasive particles and resulted in abrasive wear. The wear mode of P110 steel can be judged as oxidation wear and abrasive wear.

3.3 Corrosion resistance

The OCPs of P110 steel and G3 alloy-like coating in CO_2 -saturated simulated oilfield brine are given in Figure 10. After a certain time, both P110 steel and G3 alloy-like coating get relatively steady E_{ocp} , the value for the G3 alloy-like coating is about -0.52 V/SCE and -0.74 V/SCE for P110 steel. This confirms that the G3 alloy-like coating improves the chemical stability of P110 steel against corrosion [27].

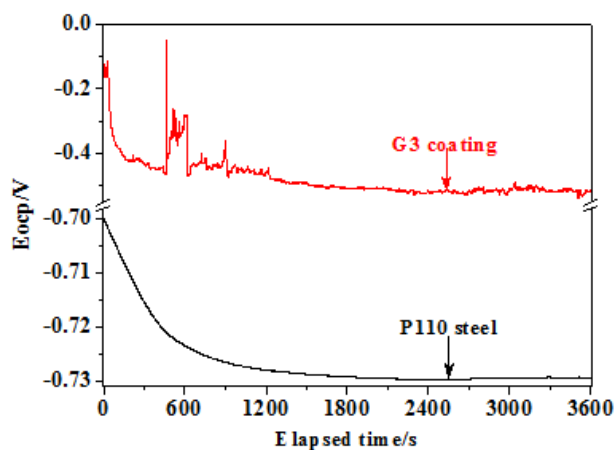


Figure 10. E_{ocp} vs. time curves of tested samples

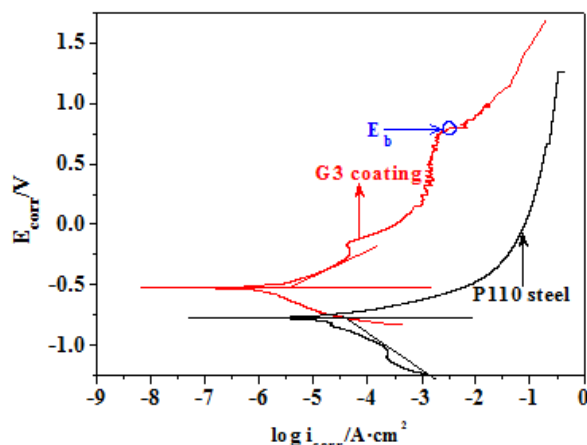


Figure 11. Polarization curves of tested samples

Figure 11 shows the potentiodynamic polarization curves of P110 steel and G3 alloy-like coating in CO₂-saturated simulated oilfield brine. Seen from Figure 11, P110 steel shows no passive zone, its anodic current increases with increasing polarization. After the polarization test of P110 steel, the corrosion medium became yellowish green, indicating the severe corrosion of P110 steel [27–31]. As shown in Figure 11, it can also be seen that the anodic branch of the polarization curve of G3 alloy-like coating is characterized by a passive region (from 0 V to 0.79 V) and breakdown potential (small circle marked). The existence of passive region for the G3 alloy-like coating reveals that the passive film has naturally formed when it was exposed to the corrosive electrolyte. By using the Tafel extrapolation method, the values corrosion current density for G3 alloy-like coating and P110 steel are 3.957×10^{-6} A/cm² and 2.505×10^{-5} A/cm², respectively [27–31]. The G3 alloy-like coating significantly enhanced the corrosion resistance of P110 steel.

4. CONCLUSIONS

In this work, continuous and compact G3 alloy-like coating has been fabricated on P110 steel by employ of DGPSA. The G3 alloy-like coating exhibited higher surface hardness value and lower mass losses than those of P110 steel. G3 alloy-like coating showed no obvious friction-reduction effect, but revealed good wear resistance with the lower mass losses. G3 alloy-like coating held higher OCP and lower current density as compared with P110 steel; it presented excellent corrosion resistance in CO₂-saturated simulated oilfield brine.

ACKNOWLEDGEMENTS

This work was supported by the Science and Technology Programs for Research and Development of Shaanxi Province (No. 2013KJXX-08), the National Natural Science Foundation of China (No. 51474154), the China Postdoctoral Science Foundation (No.2012M520604), the Natural Science Foundation for Young Scientists of Shanxi Province (No.2013021013-2, No. 2014011036-1).

References

1. A. W. Batchelor, L.N. Lam and M. Chandrasekaran, Materials Degradation and Its Control by

- Surface Engineering (3rd Edition), Imperial College Press, 1999, p.9.
2. M.L. Lepule, B.A. Obadele, A. Andrews and P.A. Olubambi, *Surf. Coat. Technol.* 261 (2015) 21.
 3. S.S. Hosmani, P. Kuppusami and R. K. Goyal, *An Introduction to Surface Alloying of Metals*, Springer, 2014, p. 1.
 4. H.L. Li, Y.P. Zhang and L.H. Han, *Steel Pipe* 36 (2007) 1.
 5. H.L. Li, Y.P. Zhang and L.H. Han, *Steel Pipe* 37 (2008) 1.
 6. J.J. Zou, N.M. Lin, L. Qin B. Tang and F.Q. Xie. *Surf. Rev. Lett.* 20 (2013) 1330002-1.
 7. Z.F. Yin, W.Z. Zhao, W.Y. Lai and X.H. Zhao. *Corro. Sci.* 51 (2009) 1702.
 8. B. Subramanian, C.V. Muraleedharan, R. Ananthakumar and M. Jayachandran, *Surf. Coat. Technol.* 205 (2011) 5014.
 9. Y.K. Chen, X.B. Zheng, Y.T. Xie, H. Ji and C.X. Ding, *Surf. Coat. Technol.* 204 (2009) 685.
 10. N.M. Lin, H.Y. Zhang, J.J. Zou and B. Tang, *Rev. Adv. Mater. Sci.* 38 (2014) 61.
 11. N.M. Lin, F.Q. Xie, T. Zhong, X.Q. Wu and W. Tian. *J. Rare Earths* 28 (2010) 301.
 12. N.M. Lin, M.L. Li, J.J. Zou, X.G. Wang and B. Tang. *J. Mater. Eng. Perform.* 22 (2013) 1365.
 13. N.M. Lin, J.W. Guo, R.Q. Hang, J.J. Zou and B. Tang, *Surf. Rev. Lett.* 21 (2014) 1450032-1.
 14. J. Xu, J.H. Ai, X.S. Xie and Z. Xu. *Surf. Coat. Technol.* 168 (2003) 142.
 15. J. Xu, J. Tao, S.Y. Jiang and Z. Xu. *Appl. Surf. Sci.* 254 (2008) 4036.
 16. X.P. Liu, K. You, K. Chen, F. Wang, Z.X. Wang and Z.Y. He. *Surf. Coat. Technol.* 228 (2013) S214.
 17. Z. Xu, X.P. Liu, P.Z. Zhang, Y.F. Zhang, G.H. Zhang and Z.Y. H, *Surf. Coat. Technol.* 201 (2007) 4822.
 18. J.J. Zou, R.Q. Hang, N.M. Lin, X.B. Huang, X.Y. Zhang, L. Qin and B. Tang. *Mod. Phys. Lett. B* 27 (2013) 1341017-1.
 19. J.J. Zou, M.L. Li, N.M. Lin, X.Y. Zhang, L. Qin and B. Tang. *Surf. Rev. Lett.* 21 (2014) 1450006-1.
 20. V. Barranco, E. Onofre, M.L. Escudero and M.C. Garcia-Alonso, *Surf. Coat. Technol.* 204 (2010) 3783.
 21. S.T. Chung and W.T. Tsai. *Thin Solid Films* 518 (2010) 7236.
 22. N.M. Lin, F.Q. Xie, T. Zhong, X.Q. Wu and W. Tian. *Adv. Mater. Res.* 79-82 (2009) 1075.
 23. N.M. Lin, F.Q. Xie, J. Zhou, X.Q. Wu and W. Tian. *J. Wuhan Univ. Technol. Mater. Sci. Ed.* 26 (2011) 191.
 24. T.Y. Cho, J.H. Yoon, Y.K. Joo, S.H. Zhang, J.Y. Cho, J.H. Kang, H.G. Chun, S.C. Kwon and M.X. Li, *Surf. Rev. Lett.* 17 (2010) 207.
 25. N.M. Lin, F.Q. Xie, H.J. Yang, W. Tian, H.F. Wang and B. Tang. *Appl. Surf. Sci.* 258 (2012) 4960.
 26. N.M. Lin, F.Q. Xie, J. Zhou, T. Zhong, X.Q. Wu and W. Tian. *J. Cent. South Univ. Technol.* 17 (2010) 1155.
 27. J. Liang, S.P. Bala, C. Blawert, M. Störmer and W. Dietzel, *Electrochim. Acta* 54 (2009) 3842.
 28. N.M. Lin, P. Zhou, Y.T. Wang, J.J. Zou, Y. Ma, Z.X. Wang, W. Tian, X.F. Yao and Bin Tang. *Surf. Rev. Lett.* 22 (2015) 1550033-1.
 29. J.J. Zou, F.Q. Xie, N.M. Lin, X.F. Yao, W. Tian and B. Tang. *Surf. Rev. Lett.* 20 (2013) 1350041-1.
 30. N.M. Lin, H.Y. Zhang, J.J. Zou, P.J. Han, Y. Ma and B. Tang. *Int. J. Electrochem. Sci.* 10 (2015) 356.
 31. N.M. Lin, P. Zhou, H.W. Zhou, J.W. Guo, H.Y. Zhang, J.J. Zou, Y. Ma, P.J. Han and Bin Tang. *Int. J. Electrochem. Sci.* 10 (2015) 2694.